

Analysis of rotation curves in the framework of R^n gravity

C. Frigerio Martins[★] and P. Salucci[★]

Astroparticle, Astrophysics Sectors, Scuola Internazionale Superiore di Studi Avanzati (SISSA), Via Beirut 4, 34014 Trieste, Italy

Accepted 2007 July 26. Received 2007 July 17; in original form 2007 March 12

ABSTRACT

We present an analysis of a devised sample of rotation curves (RCs), with the aim of checking the consequences of a modified $f(R)$ gravity on galactic scales. Originally motivated by the mystery of dark energy, this theory may explain the observed non-Keplerian profiles of galactic RCs in terms of a breakdown of Einstein general relativity. We show that, in general, the power-law $f(R)$ version could fit the observations well, with reasonable values for the mass model parameters. This could encourage further investigation into R^n gravity from both observational and theoretical points of view.

Key words: gravitation – galaxies: kinematics and dynamics – dark matter.

1 INTRODUCTION

It is well known that the rotation curves (RCs) of spiral galaxies show a non-Keplerian circular velocity profile, which cannot be explained by considering a Newtonian gravitational potential generated by baryonic matter (Persic, Salucci & Stel 1996). Currently, possible explanations, among others, for this problem are the postulate of a new, yet not detected, state of matter, dark matter (Rubin 1983), a phenomenological modification of Newtonian dynamics (Milgrom 1983; Sanders & McGaugh 2002; Brownstein & Moffat 2006; Bekenstein 2006) and higher-order gravitational theories (originally devoted to solving the dark energy issue; see, for example, Capozziello et al. 2004; Carroll et al. 2004).

In the recent theory proposed by Capozziello, Cardone & Troisi (2007, hereafter CCT), the usual Newtonian potential generated by baryonic matter is modified in such a way that the predicted and observed galaxy kinematics are in much better agreement. CCT consider power-law fourth-order¹ theories of gravity, obtained by replacing in the action of gravity the Ricci scalar R with a function $f(R) \propto R^n$, where n is a slope parameter. The idea is that the Newtonian potential generated by a point-like source is modified to

$$\phi(r) = -\frac{Gm}{r} \left\{ 1 + \frac{1}{2} \left[(r/r_c)^\beta - 1 \right] \right\}, \quad (1)$$

where β is a function of the slope n and r_c is a scalelength parameter. It turns out that in this theory β is a universal constant while r_c depends on the particular gravitating system being studied. In a virialized system, the circular velocity is related to the derivative of the potential through $V^2 = r d\phi(r)/dr$. It is clear that equation (1) may help to explain the circular velocity observed in spirals.

We remark that any proposed solution to the galaxy RC phenomenon must not only fit the kinematics well but also, equally

important, have best-fitting values of the mass model parameters that are consistent with well-studied global properties of galaxies.

For a sample of 15 low surface brightness galaxies, the model described in CCT is fairly able to fit the RCs. However, in our view, the relevance of their finding is limited by the following considerations.

- (i) The sample contains several objects whose RCs are not smooth, symmetric and extended to large radii.
- (ii) The sample contains only low surface brightness galaxies, while a wider sample is desirable.
- (iii) The universal parameter n is not estimated by the analysis itself but is taken from other observations.

In this paper, we generalize the results of CCT and test a wider and fairer sample of spirals, improving the analysis methodology. Our goal is to perform a check of their model on galactic scales in order to investigate its consistency and universality. In Section 2, we briefly summarize the main theoretical results described in CCT, which are relevant for the analysis of our sample. In Section 3, we present our sample and the methodology of analysis. In Section 4, we present our results and finally in Section 5 we give our conclusions.

2 NEWTONIAN LIMIT OF $f(R)$ GRAVITY

The theory proposed by CCT is an example of an $f(R)$ theory of gravity (Nojiri & Odintsov 2007; Carloni, Dunsby, Capozziello & Troisi 2005). In these theories, the gravitational action is defined to be

$$S = \int d^4x \sqrt{-g} [f(R) + \mathcal{L}_m], \quad (2)$$

where g is the metric determinant, R is the Ricci scalar and \mathcal{L}_m is the matter Lagrangian. They consider

$$f(r) = f_0 R^n, \quad (3)$$

where f_0 is a constant to give correct dimensions to the action and n is the slope parameter. The modified Einstein equation is obtained by varying the action with respect to the metric components.

[★]E-mail: martins@sisssa.it; salucci@sisssa.it

¹This term comes from the fact that the generalized Einstein equations contain fourth-order derivatives of the metric.

Solving the vacuum field equations for a Schwarzschild-like metric in the Newtonian limit of weak gravitational fields and low velocities, the modified gravitational potential for the case of a point-like source of mass, m , is given by equation (1), where the relation between the slope parameter n and β (see the detailed calculation in CCT) is given by

$$\beta = \frac{12n^2 - 7n - 1 - \sqrt{36n^4 + 12n^3 - 83n^2 + 50n + 1}}{6n^2 - 4n + 2}. \quad (4)$$

Note that for $n = 1$ the usual Newtonian potential is recovered. The large- and small-scale behaviours of the total potential constrain the parameter β to be $0 < \beta < 1$.

Solution (1) can be generalized to extended systems with a given density distribution $\rho(r)$ by simply writing

$$\begin{aligned} \phi(r) &= -G \int d^3r' \frac{\rho(r')}{|\mathbf{r} - \mathbf{r}'|} \left[1 + \frac{1}{2} \left(\frac{|\mathbf{r} - \mathbf{r}'|^\beta}{r_c^\beta} - 1 \right) \right] \\ &= \phi_N(r) + \phi_C(r), \end{aligned} \quad (5)$$

where $\phi_N(r)$ represents the usual Newtonian potential and $\phi_C(r)$ is the additional correction. In this way, the Newtonian potential can be recovered when $\beta = 0$. The solution for the specific density distribution relevant for spiral galaxies is described in the following section.

3 DATA AND METHODOLOGY OF THE TEST

We selected two samples of galaxies. The first sample, with 15 galaxies, is called sample A, and represents the best available RCs to study the mass distribution of luminous and/or dark matter. It has been used in works concerning modifications of gravity and the core/cusp controversy (Gentile et al. 2004; Corbelli & Salucci 2007; Frigerio Martins & Salucci 2007).

This sample includes nearby galaxies of different surface brightnesses: DDO 47 (Gentile et al. 2005); ESO 116-G12, ESO 287-G13, NGC 7339 and 1090 (Gentile et al. 2004); UGC 8017, UGC 10981, UGC 11455 (Vogt et al. 2004); M31, M33 (Corbelli & Salucci 2007); IC 2574 (Martimbeau, Carignan & Roy 1994), NGC 5585 (Côté, Carignan & Sancisi 1991), NGC 6503 (Wevers, van der Kruit & Allen 1986), NGC 2403 (Fraternali et al. 2002), NGC 55 (Puche, Carignan & Wainscoat 1991). This sample is the most suitable for a fair test of theories such as that of CCT, for the following reasons.

- (i) The RCs are smooth, symmetric and extended to large radii.
- (ii) The galaxies present a very small bulge, which can be neglected in the mass model to a good approximation.
- (iii) The luminosity profile is well measured and presents a smooth behaviour
- (iv) The data are uniform in quality up to the maximal radii of each galaxy.

Note that in some of these galaxies H_α and H I RCs are both available, and in these cases they agree well where they coexist.

We also considered a second sample called sample B, which consists of 15 selected objects from Sanders & McGaugh (2002) and has been used to test Modified Newtonian Dynamics (MOND). This sample consists of the following galaxies: UGC 6399, UGC 6983, UGC 6917, NGC 3972, NGC 4085, NGC 4183, NGC 3917, NGC 3949, NGC 4217, NGC 3877, NGC 4157, NGC 3953, NGC 4100 (Tully et al. 1996; Verheijen & Sancisi 2001); NGC 300 (Puche, Carignan & Bosma 1990; Carignan 1985); UGC 128 (van der Hulst et al. 1993). Although these galaxies do not fulfil all the

requirements of sample A, we have analysed them for the sake of completeness. The properties of the galaxies of the two samples are listed in Table 1. Note that the theory of CCT requires an analysis with a sample of high-quality galaxies, as described above, where each luminous profile plays an important role; this is not the case in MOND.

We decompose the total circular velocity into stellar and gaseous contributions. Available photometry and radio observations show that the stars and gas in our sample of galaxies are distributed in an infinitesimal thin and circular symmetric disc. While the H I surface luminosity density distribution $\Sigma_{\text{gas}}(r)$ gives a direct measurement of the gas mass, optical observations show that the stars have an exponential distribution:

$$\Sigma_D(r) = (M_D/2\pi R_D^2) e^{-r/R_D}. \quad (6)$$

Here, M_D is the disc mass and R_D is the scalelength. The latter is measured directly from the optical observations, while M_D is kept as a free parameter of our analysis.

The distribution of the luminous matter in spiral galaxies has, to a good extent, cylindrical symmetry. Thus, using cylindrical coordinates, the potential (5) reads

$$\phi(r) = -G \int_0^\infty dr' r' \Sigma(r') \int_0^{2\pi} \frac{d\theta}{|\mathbf{r} - \mathbf{r}'|} \left[1 + \frac{1}{2} \left(\frac{|\mathbf{r} - \mathbf{r}'|^\beta}{r_c^\beta} - 1 \right) \right]. \quad (7)$$

$\Sigma(r')$ is the surface density distribution of the stars, given by equation (6), or of the gas, given by an interpolation of the H I data points up to the last measured point. β and r_c are free parameters of the theory, with the latter being galaxy-dependent. We neglected the gas contribution to the mass density for radii larger than the last measured point. However, we checked the goodness of this approximation by extending the distribution with a different type of decreasing smooth curve and we realized that the error made in the truncated approximation is small enough to be neglected.

Defining $k^2 \equiv \frac{4r'}{(r+r')^2}$, we can express the distance between two points in cylindrical coordinates as $|\mathbf{r} - \mathbf{r}'| = (r+r')[1 - k^2 \cos^2(\theta/2)]$. The derivation of the circular velocity due to the marked term of equation (7), which we call $\phi_\beta(r)$, is now direct:

$$r \frac{d}{dr} \phi_\beta(r) = -2^{\beta-3} r_c^{-\beta} \pi \alpha (\beta - 1) G I(r). \quad (8)$$

Here, the integral is defined as

$$\mathcal{I}(r) \equiv \int_0^\infty dr' r' \frac{\beta - 1}{2} k^{3-\beta} \Sigma(r') \mathcal{F}(r), \quad (9)$$

with $\mathcal{F}(r)$ written in terms of the confluent hyper-geometric function: $\mathcal{F}(r) \equiv 2(r+r') {}_2F_1[\frac{1}{2}, \frac{1-\beta}{2}, 1, k^2] + [(k^2 - 2)r' + k^2 r] {}_2F_1[\frac{3}{2}, \frac{3-\beta}{2}, 2, k^2]$

The total circular velocity is the sum of each squared contribution:

$$V_{\text{CCT}}^2(r) = V_{\text{N,stars}}^2 + V_{\text{N,gas}}^2 + V_{\text{C,stars}}^2 + V_{\text{C,gas}}^2. \quad (10)$$

Here, the subscripts ‘stars’ and ‘gas’ refer to the different contributions of luminous matter to the total potential (5). The subscripts ‘N’ and ‘C’ refer to the Newtonian and the additional correction potentials.

Let us recall that we can write

$$V_{\text{N,stars}}^2(r) = (GM_D/2R_D)x^2 B(x/2), \quad (11)$$

where $x \equiv r/R_D$, G is the gravitational constant and the quantity $B = I_0 K_0 - I_1 K_1$ is a combination of Bessel functions (Freeman 1970).

Galaxies UGC 8017, M31, UGC 11455 and UGC 10981 present

Table 1. Properties and parameters of the mass model of the analysed samples ($\beta = 0.7$). From left to right, the columns show: the name of the galaxy, the Hubble type, as reported in the NASA/IPAC Extragalactic Database (NED), the adopted distance in Mpc, the B -band luminosity in $10^9 L_{B\odot}$, the disc scalelength in kpc, the gas mass in $10^9 M_\odot$ up to the last measured point, the gas fraction in per cent, the disc mass in $10^9 M_\odot$, the scalelength CCT parameter in kpc, the mass-to-light ratio in Υ_\odot^B , and χ_{red}^2 . The galaxies are ordered from top to bottom with increasing luminosity.

| Galaxy | Type | D | L_B | R_D | M_{gas} | f_{gas} | M_D | r_c | Υ_\star^B | χ_{red}^2 |
|-------------|-------|-------|-------|-------|------------------|------------------|---------------|-------------------|--------------------|-----------------------|
| Sample A | | | | | | | | | | |
| DDO 47 | IBm | 4 | 0.1 | 0.5 | 2.2 | 96 ± 1 | 0.01 | 0.005 | 0.1 | 0.5 |
| IC 2574 | SABm | 3 | 0.8 | 1.78 | 0.52 | 79 ± 12 | 0.14 | 0.017 ± 0.003 | 0.2 | 0.8 |
| NGC 5585 | SABc | 6.2 | 1.5 | 1.26 | 1.45 | 58 ± 3 | 1 | 0.038 ± 0.004 | 0.7 | 1.4 |
| NGC 55 | SBm | 1.6 | 4 | 1.6 | 1.3 | 84 ± 7 | 0.24 | 0.024 ± 0.004 | 0.06 | 0.14 |
| ESO 116-G12 | SBm | 15.3 | 4.6 | 1.7 | 21 | 50 | 2.1 | 0.05 ± 0.01 | 0.5 | 1.2 |
| NGC 6503 | Sacd | 6 | 5 | 1.74 | 2.3 | 18 ± 0.7 | 10.6 | 0.21 ± 0.014 | 2.1 | 18 |
| M33 | Sacd | 0.84 | 5.7 | 1.4 | 3.7 | 53 ± 2 | 3.3 | 0.075 ± 0.004 | 0.58 | 25 |
| NGC 7339 | SABbc | 17.8 | 7.3 | 1.5 | 6.2 | 2.8 ± 0.2 | 22 | 0.41 ± 0.07 | 3 | 2.3 |
| NGC 2403 | SABcd | 3.25 | 8 | 2.08 | 4.46 | 27 ± 0.9 | 12.1 | 0.21 ± 0.015 | 1.5 | 19 |
| M31 | SAB | 0.78 | 20 | 4.5 | – | – | 180 ± 70 | 1.53 ± 0.19 | 9 | 3.4 |
| ESO 287-G13 | Sc | 35.6 | 30 | 3.3 | 14 | 25 ± 1 | 41 | 0.48 ± 0.05 | 1.4 | 3.2 |
| NGC 1090 | SBbc | 36.4 | 38 | 3.4 | 100 | 18 ± 1 | 47 | 0.59 ± 0.04 | 1.2 | 0.9 |
| UGC 8017 | Sab | 102.7 | 40 | 2.1 | – | – | 9.1 ± 0.3 | 0.01 ± 0.01 | 0.23 | 5.2 |
| UGC 11455 | Sc | 75.4 | 45 | 5.3 | – | – | 74 ± 3 | 0.14 ± 0.01 | 1.6 | 5 |
| UGC 10981 | Sbc | 155 | 120 | 5.4 | – | – | 460 ± 200 | $\sim 10^{11}$ | 3.8 | 4.9 |
| Sample B | | | | | | | | | | |
| UGC 6399 | Sm | 18.6 | 1.6 | 2.4 | 1 | 23 ± 3 | 3.3 | 0.1 ± 0.03 | 2 | 0.1 |
| NGC 300 | SACd | 1.9 | 2.3 | 1.7 | 1.3 | 39 ± 4 | 2 | 0.052 ± 0.010 | 0.87 | 0.43 |
| UGC 6983 | SBcd | 18.6 | 4.2 | 2.7 | 4.1 | 24 ± 2 | 13 | 0.46 ± 0.1 | 3.1 | 0.88 |
| UGC 6917 | SBm | 18.6 | 4.4 | 2.9 | 2.6 | 14 ± 1 | 16 | 0.71 ± 0.17 | 3.6 | 0.47 |
| UGC 128 | Sdm | 60 | 5.2 | 6.4 | 10.7 | 32 ± 5 | 23 | 0.39 ± 0.11 | 4.4 | 0.1 |
| NGC 3972 | SABc | 18.6 | 6.7 | 2 | 1.5 | 39 ± 3 | 2.5 | 0.025 ± 0.004 | 0.37 | 0.1 |
| NGC 4085 | SABc | 18.6 | 6.9 | 1.6 | 1.3 | 44 ± 4 | 1.7 | 0.014 ± 0.003 | 0.25 | 1 |
| NGC 4183 | SACd | 18.6 | 9.5 | 1.4 | 4.9 | 60 ± 6 | 3.2 | 0.09 ± 0.023 | 0.3 | 0.33 |
| NGC 3917 | SACd | 18.6 | 11 | 3.1 | 2.6 | 22 ± 1.5 | 9.2 | 0.098 ± 0.014 | 0.8 | 1 |
| NGC 3949 | SABc | 18.6 | 19 | 1.7 | 4.1 | 19 ± 2.2 | 17 | 0.22 ± 0.06 | 0.9 | 0.25 |
| NGC 4217 | SAB | 18.6 | 21 | 2.9 | 3.3 | 6.1 ± 0.7 | 52 | 0.55 ± 0.15 | 2.5 | 0.38 |
| NGC 4100 | SABc | 18.6 | 25 | 2.5 | 4.4 | 13 ± 1.5 | 28 | 0.20 ± 0.03 | 1.1 | 1.52 |
| NGC 3877 | Sc | 18.6 | 27 | 2.8 | 1.9 | 7.3 ± 0.8 | 24 | 0.2 ± 0.04 | 0.9 | 0.75 |
| NGC 4157 | SABb | 18.6 | 30 | 2.6 | 12 | 26 ± 2.6 | 33 | 0.25 ± 0.04 | 1.1 | 0.53 |
| NGC 3953 | Sbbc | 18.6 | 41 | 3.8 | 4 | 2.8 ± 0.18 | 140 | 1.9 ± 0.5 | 3.4 | 0.78 |

a very small amount of gas, and for this reason have been neglected in the analysis. Notice that the correction to the Newtonian potential in equation (1) may be negative and this would lead to a negative value of V_C^2 . In Figs 1 and 2, however, the velocities V_C are shown only in the ranges of r where their squares are positive.

As a first step, the RCs are χ^2 best-fitted with the following free parameters: the slope (β) and the scalelength (r_c) of the theory, and the gas mass fraction (f_{gas}) related to the disc mass simply by $M_D = M_{\text{gas}}(1 - f_{\text{gas}})/f_{\text{gas}}$. The errors for the best-fitting values of the free parameters are calculated at one standard deviation with the $\chi_{\text{red}}^2 + 1$ rule. From the results of these fits, we obtain a mean value of $\beta = 0.7 \pm 0.25$ ($n \simeq 2.2$). As the second step, we again perform the best-fitting, fixing the slope parameter at $\beta = 0.7$ and keeping as free parameters only r_c and f_{gas} . Note that in a previous paper (Capozziello, Cardone & Troisi 2006) a mean value of $\beta = 0.58 \pm 0.15$ ($n \simeq 1.7$) was obtained, perfectly compatible with our result. This parameter, however, is well constrained from Type Ia supernovae observations to be $\beta = 0.87$ ($n \simeq 3.5$), also compatible with our measurements. In our analysis, the value $\beta = 0.7$ is the most favourable for explaining the RCs; different values of β from that we adopt here lead to worse performance.

4 RESULTS

We summarize the results of our analysis in Figs 1 and 2 and Table 1.² In general, for all galaxies we find the following:

- (i) the velocity model V_{CCT} that fits the RCs well;
- (ii) acceptable values for the stellar mass-to-light ratio;
- (iii) a range too vast for values of the gas fraction ($0 < f_g < 100$ per cent);
- (iv) no clear understanding of the large variation of values for the scalelength parameter ($0.005 < r_c < 1.53$ kpc).

The residuals of the measurements with respect to the best-fitting mass model are in most cases compatible with the error bars (see Figs 1 and 2), although three galaxies (NGC 6503, NGC 2403 and M33) show significant deviations. We also find acceptable values for the B -band mass-to-light ratio parameter for most of the galaxies. For this, we should have approximately $0.5 < \Upsilon_\star^B < 6$ and a positive

² The numerical codes and data used to obtain these results can be found at <http://people.sissa.it/~martins/home.html>.

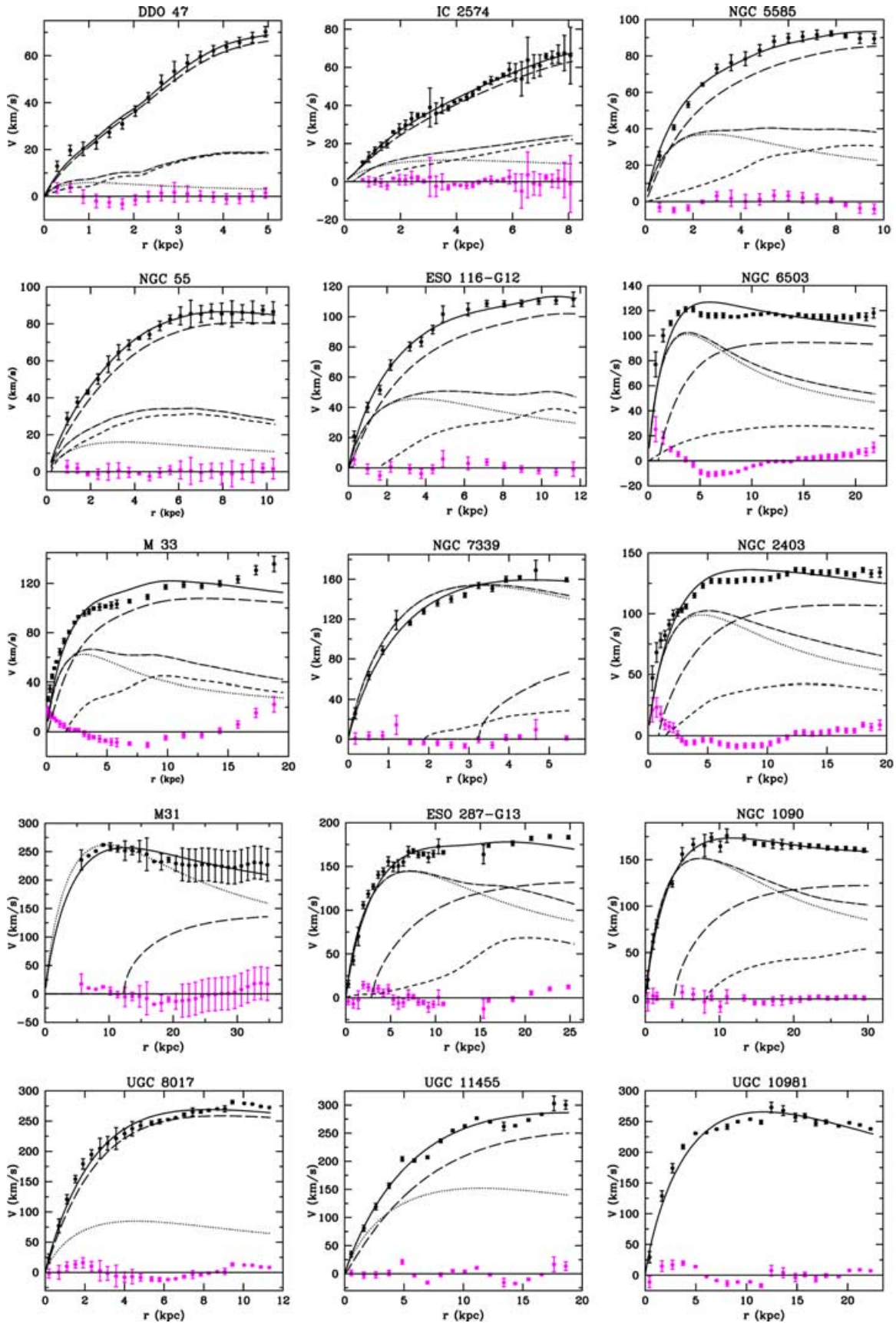


Figure 1. Sample A. The solid line represents the best-fitting total circular velocity V_{CCT} . The dashed and dotted lines are the Newtonian contributions from the gas and the stars, while the dot-dashed line represents their sum. The long-dashed line is the non-Newtonian contribution of the gas and the stars to the model. Below the RCs, we plot the residuals ($V_{obs} - V_{CCT}$). See Table 1 for details.

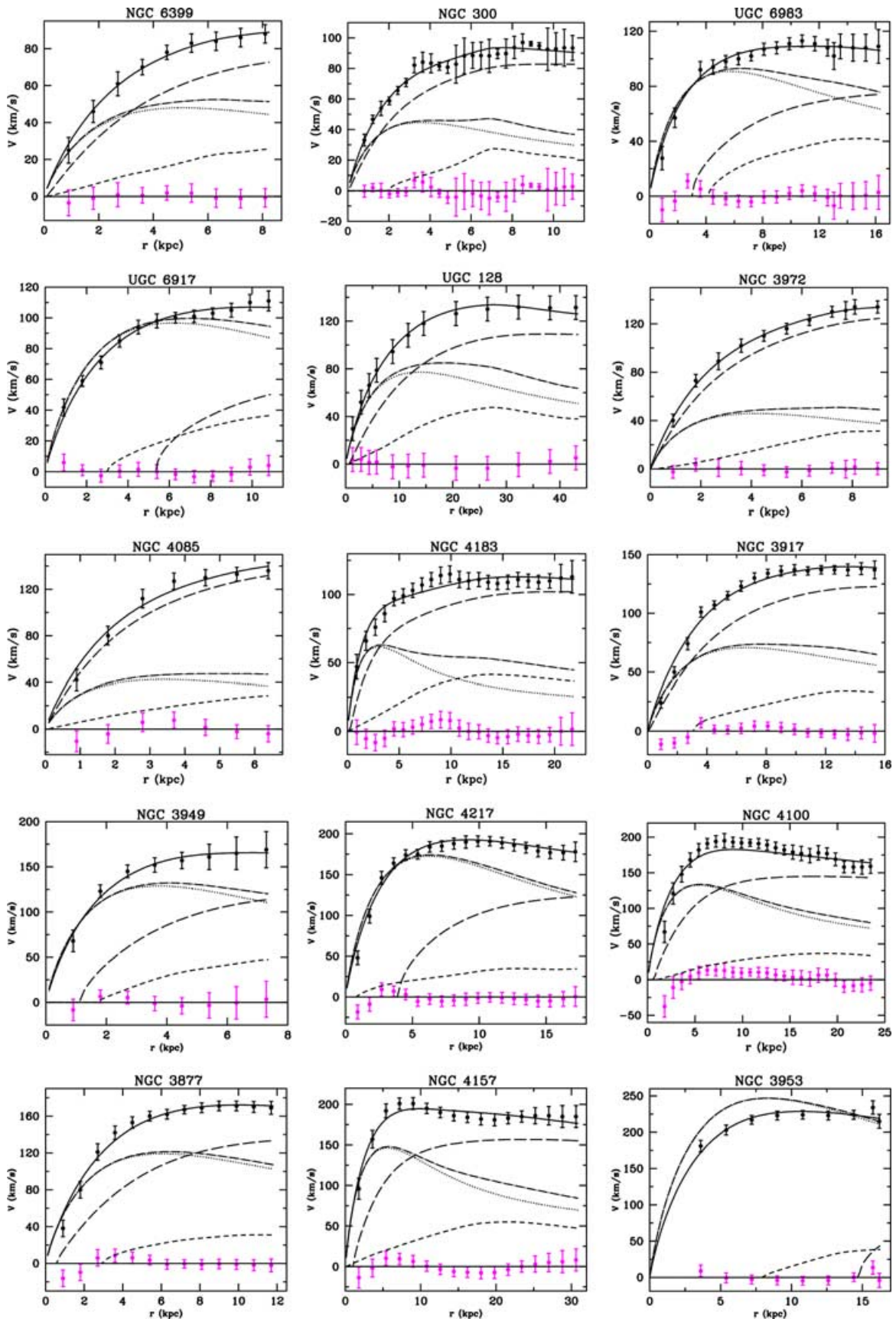


Figure 2. Sample B. Best-fitting curves superimposed to the data from selected objects from Sanders & McGaugh (2002). See Fig. 1 for details.

correlation between B luminosity³ and Υ_{\star}^B (Salucci & Persic 1999):

$$M_D(L_B) \simeq 3.7 \times 10^{10} \times \left[\left(\frac{L_B}{L_{10}} \right)^{1.23} g(L_B) + 0.095 \left(\frac{L_B}{L_{10}} \right)^{0.98} \right] M_{\odot}. \quad (12)$$

Here, $L_{10} \equiv 10^{10} L_{B\odot}$ and

$$g(L_B) = \exp \left[-0.87 \times \left(\log \frac{L_B}{L_{10}} - 0.64 \right)^2 \right].$$

In detail, we find discrepancies for NGC 55, UGC 8017, NGC 3972, NGC 4085 and NGC 4183. Values for the scalelength parameter (r_c) are in general smaller for less massive galaxies and larger for more massive galaxies. We obtained a Newtonian fit for UGC 10981, as shown by the exceedingly large value for r_c (see Fig. 1).

The model analysed here yields better results on galactic scales than cold dark matter numerical simulations, where in the latter these galaxies have serious problems with marginal fits and unreasonable values for the stellar mass-to-light ratio; see, for example, Gentile et al. (2004); Frigerio Martins & Salucci (2007).

5 CONCLUSIONS

We have investigated the possibility of fitting the RCs of spirals with the power-law fourth-order theory of gravity of CCT, without the need for dark matter. We remark on the relevance of our sample, which contains objects in a large range of luminosities and with very accurate and proper kinematics. We find, in general, reasonable agreement, with some discrepancies, between the RCs and the CCT circular velocity model, encouraging further investigations from a theoretical point of view.

³ $\Upsilon_{\star}^B \equiv M_D/L_B$; M_D is the disc mass and L_B is the B -band galaxy luminosity.

ACKNOWLEDGMENTS

We warmly thank S. Capozziello, J. Miller and T. Sotiriou for useful discussions. This research was supported by CAPES-Brasil (CFM).

REFERENCES

- Bekenstein J. D., 2006, *Contemporary Physics*, 47, 387
 Brownstein J. R., Moffat J. W., 2006, *ApJ*, 636, 721
 Capozziello S., Cardone V. F., Carloni S., Troisi A., 2004, *Phys. Lett. A*, 326, 292
 Capozziello S., Cardone V. F., Troisi A., 2006, *JCAP*, (8), 001
 Capozziello S., Cardone V. F., Troisi A., 2007, *MNRAS*, 375, 1423 (CCT)
 Carignan C., 1985, *ApJS*, 58, 107
 Carloni S., Dunsby P. K. S., Capozziello S., Troisi A., 2005, *Class. Quant. Grav.*, 22, 4839
 Carroll S., Duvvuri V., Trodden M., Turner M. S., 2004, *Phys. Rev. D*, 70, 043528
 Corbelli E., Salucci P., 2007, *MNRAS*, 374, 1051
 Côté S., Carignan C., Sancisi R., 1991, *AJ*, 102, 904
 Fraternali F., van Moorsel G., Sancisi R., Oosterloo T., 2002, *AJ*, 123, 3124
 Freeman K. C., 1970, *ApJ*, 160, 811
 Frigerio Martins C., Salucci P., 2007, *Phys. Rev. Lett.*, 98, 151301
 Gentile G., Salucci P., Klein U., Vergani D., Kalberla P., 2004, *MNRAS*, 351, 903
 Gentile G., Burkert A., Salucci P., Klein U., Walter F., 2005, *ApJ*, 234, L145
 Martimbeau N., Carignan C., Roy J., 1994, *AJ*, 107, 543
 Milgrom M., 1983, *ApJ*, 270, 365
 Nojiri S., Odintsov S. D., 2007, *IJGMMP*, 4, 115
 Persic M., Salucci P., Stel F., 1996, *MNRAS*, 281, 27
 Puche D., Carignan C., Wainscoat R. J., 1991, *AJ*, 101, 447
 Puche D., Carignan C., Bosma A., 1996, *AJ*, 100, 1468
 Rubin V. C., 1983, *Sci.*, 220, 1339
 Salucci P., Persic M., 1999, *MNRAS*, 309, 923
 Sanders R. H., McGaugh S. S., 2002, *ARA&A*, 40, 263
 Tully R. B., Verheijen M. A. W., Pierce M. J., Huang J., Wainscoat R. J., 1996, *AJ*, 112, 2471
 van der Hulst J. M., Skillman E. D., Smith T. R., Bothun G. D., McGaugh S. S., de Blok W. J. G., 1993, *AJ*, 106, 548
 Verheijen M. A. W., Sancisi R., 2001, *A&A*, 370, 765
 Vogt N. P., Haynes M. P., Herter T., Giovanelli R., 2004, *AJ*, 127, 3273
 Wevers B. M. H. R., van der Kruit P. C., Allen R. J., 1986, *A&A*, 4, 86

This paper has been typeset from a $\text{\TeX}/\text{\LaTeX}$ file prepared by the author.